



BMP6 binding to heparin and heparan sulfate is mediated by N-terminal and C-terminal clustered basic residues

Andrea Denardo^{a,1}, Stefano Elli^{b,1}, Stefania Federici^c, Michela Asperti^a, Magdalena Gryzik^a, Paola Ruzzenenti^a, Fernando Carmona^a, Paolo Bergese^a, Annamaria Naggi^b, Paolo Arosio^a, Maura Poli^{a,*}

^a Department of Molecular and Translational Medicine, University of Brescia, Viale Europa 11, 25123 Brescia, Italy

^b G. Ronzoni Institute for Chemical and Biochemical Research, Via Giuseppe Colombo 81, 20133 Milan, Italy

^c Department of Mechanical and Industrial Engineering and INSTM, University of Brescia, Via Branze 38, 25123 Brescia, Italy

ARTICLE INFO

Keywords:

Bone morphogenetic protein 6 (BMP6)
Hepcidin
Heparin
Heparan sulfate
Interaction

ABSTRACT

Background: The bone morphogenetic protein 6 (BMP6) is a crucial inducer of hepcidin, the peptide hormone that regulates the iron availability in our body. Hepcidin expression is influenced by hepatic heparan sulfate (HS) and by heparin administration, suggesting BMP6 interaction with heparin/HS. The BMP2/4 subfamily has been deeply characterized to have a N-terminal heparin/HS binding domain (HBD), whose basic residues contact the sulfate groups on heparin and HS. Such detailed characterization is still required for other, structurally different BMPs, including BMP6.

Methods: BMP6 peptides encompassing potential HBDs were analysed on heparin-functionalized plates and microcantilevers, and on membrane HS expressing CHO-K1 cells. Monomeric wild-type BMP6 and mutants were produced, substituting the basic residues with non-charged ones, and their affinity to the heparin-column was measured. The BMP6-heparin interaction was also predicted at atomic level by *in silico* molecular dynamics.

Results: N-terminal and C-terminal BMP6 peptides showed high heparin affinity in solid-phase assays. The mutation of the two sites (R5L, R6S, R7L and K126N, K127N, R129S) abolished the heparin-binding activity of the recombinant monomeric BMP6. Monomeric BMP6 and peptides specifically bound to membrane HS of CHO-K1 cells through the same domains. Molecular dynamic studies supported the role of the two HBDs, suggesting a cooperative behaviour.

Conclusions: In BMP6, N-terminal (R5, R6, R7) and C-terminal (K126, K127, R129) domains mediate the interaction with heparin and HS.

General significance: This study provides the molecular mechanism supporting the use of heparin to sequester BMP6 and inhibit hepcidin expression, a novel clinical approach for high-hepcidin iron disorders.

1. Introduction

The bone morphogenetic proteins (BMPs) represent the largest subgroup of the transforming growth factor- β superfamily, that includes over 20 members in human [8]. They are all synthesized as pro-protein precursors undergoing proteolytic cleavage to generate the mature chains that then assemble into dimers, functional in binding the BMP

receptors to elicit cellular signalling. After binding the ligand, the receptors complex phosphorylates the downstream effectors SMAD1/5/8, which then associate with SMAD4 and translocate into the nucleus to induce the expression of several genes [25,26,58]. Despite the common mechanism of signalling, BMPs are involved in different biological processes of development and homeostasis, beyond the osteogenic function that was firstly described [56]. BMPs activities can be

Abbreviations: BMP6, Bone morphogenetic protein 6; GAG, Glycosaminoglycans; HS, Heparan sulfate; CS, Chondroitin sulfate; DS, Dermatan sulfate; HSPG, heparan sulfate proteoglycans; HBD, Heparin/HS-binding domain; MD, Molecular Dynamic; SEC-TDA, Size exclusion chromatography followed by a triple detector array.

* Corresponding author.

E-mail address: maura.poli@unibs.it (M. Poli).

¹ Equal contribution.

<https://doi.org/10.1016/j.bbagen.2020.129799>

Received 1 July 2020; Received in revised form 16 November 2020; Accepted 18 November 2020

Available online 21 November 2020

0304-4165/© 2020 Elsevier B.V. All rights reserved.

modulated by other molecules, among which the heparan sulfate (HS) glycans, that were shown to influence the spatial control and protein-protein interactions of some BMPs [51].

All the animal cells express heparan sulfate proteoglycans (HSPGs), glycoproteins that contain one or more HS polysaccharide chains linked to the proteoglycan protein core [7,38]. The HS chain is made of repeated disaccharidic units of *N*-acetyl-glucosamine (GlcNAc) and glucuronic acid (GlcA), linked by a 1–4 glycosidic bond. During their assembly, the HS chains undergo a series of processing reactions involving GlcNAc *N*-deacetylation and *N*-sulfation, epimerization of GlcA to iduronic acid (IdoA), and *O*-sulfation that generate relatively short segments of modified sugars interspersed by variable tracts of unmodified sugars [15]. Heparin is considered part of this group of glycans, although it is an unusually short and highly sulfated HS chain [37].

BMPs were initially purified on heparin columns, but the interaction with heparin/HS has been well-characterized mainly for BMP2 and BMP4: the heparin/HS-binding domains (HBDs) were identified as *N*-terminal cores rich in basic residues, that contact the negatively charged sulfate groups displayed by heparin/HS [42,52]. This interaction is biologically relevant, since heparin prevents BMP2 binding to BMP receptors inhibiting the osteogenic activity [33], while membrane-bound HS facilitates the BMP2-induced BMP receptor complex formation *in vitro* [35] and regulates BMP4 action range in *Xenopus* embryo [42].

BMP6 belongs to a BMP subfamily different from that of BMP2/4 and its HBDs are yet to be established [51]. BMP6 plays a major role in bone formation [56] but it is also a key player in systemic iron homeostasis, since it is the major inducer of the hepatic expression of the peptide hormone hepcidin that regulates systemic iron availability [1,10]. Interestingly, exogenous heparin administration inhibits BMP6 biological activities both as osteogenic factor [9] and as hepcidin inducer [3,45–48], while the alteration of endogenous hepatic HS specifically downregulates the BMP/SMAD signalling and hepcidin expression [4,49]. Altogether these observations showed that a glycan-protein interaction influences BMP6 function. The difficulties to produce the full-length BMP6 as soluble recombinant folded protein [54] likely dampened detailed studies of its interaction with heparin/HS. Consequently only a recent report by Billings et al. investigated this aspect using BMP6 peptides that led to the identification of a novel HBD located near the C-terminus [6].

In our present work, we investigated the BMP6 activity in binding heparin and HS using different approaches. We identified clusters of basic residues as putative interaction sites and the corresponding synthetic peptides were studied for heparin and HS binding in solid-phase assays to identify two major domains. Then, the full-length human monomeric BMP6 was expressed in *E. coli* and assessed to interact with heparin and HS. The substitution of basic residues with neutral ones in two putative HBDs, located near the C-terminus and the N-terminus, strongly reduced the heparin interaction. In addition, *in silico* study of BMP6-heparin interaction confirmed the *in vitro* observation and proposed the atomic details of possible molecular recognition and contact sites among BMP6 and a representative heparin chain. The results confirm and extend the recent findings by Billings and colleagues [6].

2. Methods

2.1. BMP6 peptides

Linear peptides, corresponding to BMP6 arginine and lysine rich domains, were synthesized by Thermo Fisher Scientific custom peptide service (Table 1). A *N*-terminal biotin tag was linked to each peptide, allowing the detection during the binding *in vitro* assays.

2.2. Heparin-coated plate assay

Immunosorbent 96-well plate (immunoGRADE, BRANDplates®) was

Table 1

BMP6 peptides representing potential heparin/HS-binding domains (HBDs). Sequence and numbers of amino acids, molecular weight and isoelectric point (pI) of the *N*-terminal biotin-tagged synthetic peptides, analysed during *in vitro* heparin-binding assays.

BMP6 peptide	Sequence	Amino acid number	Molecular weight (Da)	pI
HBD1	[Btn] SRRRQQSRNRSTQS [COOH]	14	1973	12.6
HBD1 mutant	[Btn] SLSLQQSRNRSTQS [COOH]	14	1818	12.0
HBD2	[Btn] LKTACRKHELY [COOH]	11	1588	9.2
HBD3	[Btn] LKKYRNMMVVRACGCH [COOH]	15	2005	9.9
HBD3 mutant	[Btn] LNNYSNMVVRACGCH [COOH]	15	1907	8.1

coated with 10 µg/mL protamine salt from salmon (no. P4020, Sigma) in 50 mM carbonate buffer pH 9.6, overnight at 4 °C, generating a first cationic-polypeptide coating layer for the subsequent heparin functionalization. Unfractionated high molecular weight heparin from porcine mucosal heparin (17.6 kDa, degree of sulfation 2.4 SO₃/COO⁻, 14.3% NAc) was resuspended in phosphate buffer saline +0.1% tween20 (PBST) + 1% bovine serum albumin (BSA) at concentration of 20 µg/mL, spotted onto the plate and incubated overnight at 4 °C. The non-specific binding sites were saturated with PBST +3% BSA and the plate was incubated with different concentrations of synthetic BMP6 peptides (5, 25, 50, 250, 2500 nM, in PBST +1% BSA), overnight at 4 °C. Unbound molecules were removed rinsing three times the plate with PBST. The presence of biotinylated BMP6 peptides was detected incubating with streptavidin-horseradish peroxidase (HRP) conjugated (220 ng/mL in PBST +1% BSA, no. S2438, Sigma). Finally, the signal was developed by chromogenic HRP-substrate TMB incubation (prepared according to the manufacturer's instruction, no. T2885, Sigma-Aldrich), stopped by 1 N H₂SO₄ and detected at 405 nm emission wavelengths using a Multiskan®EX plate reader (Thermo Scientific). The resulting values were analysed with Sigma plot (v 11.0) by non-linear regression, ligand binding, one-site saturation, curve fitting.

2.3. Microcantilever heparin-binding assay

Arrays of eight Silica Microcantilevers (MCs), 500 × 100 × 1 µm³ were coated with a 20 nm thin gold film on their top faces (Concentris GmbH, Basel, Switzerland) that allows a selective use of thiol chemistry. Cystamine (thiol) reducing end derivatization of heparin was performed. Briefly, heparin (75 mg/mL in 15 mM phosphate buffer pH 8.1) was mixed to Cystamine (12 mg/mL), heated up to 40 °C and stirred for 1 h. NaBH₃CN (9.8 mg/mL) was added to the mixture and stirred at 40 °C for 24 h. An additional amount of NaBH₃CN (9.8 mg/mL) was added heating the mixture for a further 24 h. The reaction mixture was diluted with H₂O and dialyzed for 48 h. The sample was concentrated and purified by size exclusion chromatography on G-10 Sephadex using H₂O/ethanol (9:1 vol:vol ratio). The cystamine derivative of heparin was obtained with 85% (w/w) yield. The percentage of amino group attached to the reducing end was confirmed by ¹H NMR and molecular weight evaluated by SEC-TDA (MW = 20,700 Da) analysis. Prior to heparin functionalization, the MCs were washed 30 min with acetone and then 30 min with ozone-UV. Next, each MC was immersed in a capillary tube delivering 1 mg/mL thiolated heparin in 0.1 M HEPES pH 6.5 buffer, for 4 h. Four out of eight MCs were functionalized with thiolated heparin, while the remaining four were not functionalized, as negative controls. BMP6 peptides loading experiments were performed by the Cantisens Research MC platform (Concentris GmbH, Basel, Switzerland), which is equipped with a microfluidic system to handle

Table 2
Primers for human BMP6 site-directed mutagenesis. Amino acid substitutions in BMP6 and the corresponding HBD are indicated in the first and second column, respectively. Forward and reverse mutagenesis primers are reported in the second and third column. The varying nucleotides are in bold.

Mutation	BMP6 domain	Mutagenesis primer forward (5'→3')	Mutagenesis primers reverse (5'→3')
R5L R6S R7L	HBD1	CCACTCAGCCTCCAGCCTGAGCCTACAACACAGAGTGTATC	GATTACGACTCTCTTAGGCTCAGGCTGGAGGCTCAGTGG
R39S K40N	HBD2	GAAITGAAACAACAGCCTGGCAGCAATCATGAGCTGTATGTGAGTTTC	GAAACTCACATACAGGCTCATGTTGTGCGAGGCTGTTTTCAAATTC
K126N K127N R129S	HBD3	CCACAAGCTCTTACAACCATATTGCTCTAATTATTCAGAATGACATTGGAGTTGTC	GACAACTCCAATGCTCATCTTCTGAAATAATTACAGCAATATGGTTGTAAGAGCTTGTGG

liquid delivery of the BMP6 peptides to the MCs at a flux rate of 0.42 $\mu\text{L}/\text{s}$, a multiple lasers for simultaneous measurement of the individual MC deflection and an integrated temperature controller to allow measurements at the stable temperature of 25 °C. MC arrays were equilibrated under 0.1 M HEPES pH 6.5 buffer at 25 °C for about 3 h before the injection of the BMP6 peptide sample. HBD1 and HBD3 peptides (Table 1) were injected at different concentrations (0.5, 5, 10, 25, 50 μM) in milli-Q water.

2.4. Glycosaminoglycans competition with BMP6-heparin binding

Heparin-coated plates were prepared as reported above. BMP6 biotinylated peptides (50 nM in PBST +1% BSA) were incubated for 2 h at RT, with varying concentrations (0.4, 1.2, 3.6, 11 $\mu\text{g}/\text{mL}$) of different glycosaminoglycans (GAGs), whose sulfation degree was estimated by integration of the NMR spectra [40]: porcine mucosa derived unfractionated heparin (2.4 sulfates per disaccharide), partially desulfated heparins Hep 2-O DeS (1.82 sulfates per disaccharide, 20.0% residual 2-O sulfation) and Hep 6-O DeS (1.67 sulfates per disaccharide, 7.4% residual 2-O sulfation), chondroitin sulfate (CS) (0.9 sulfates per disaccharide) and dermatan sulfate (DS) (1.1 sulfate per disaccharide) as described by Poli et al. [46]. All were resuspended in PBST +1% BSA. After pre-incubation, the mixtures of biotinylated peptides-GAGs were analysed on heparin-coated plate for binding, as previously described.

2.5. Cloning of human mature BMP6 cDNA into pASK-IBA43plus vector

The human mature BMP6 coding sequence was PCR amplified from the cDNA of HepG2 hepatoma cell line, using a 5' overhanging primer pair to introduce *NheI* and *HindIII* restriction sites and an in-frame histidine (6xHis) tag coding sequence. The amplification product was cloned into a pASK-IBA43plus plasmid vector (IBA-lifesciences) under the control of inducible "tet" promoter, using the mentioned restriction enzymes (Promega, cod. R6501 and cod. R6041). The so-obtained plasmid construct (pASK h-BMP6) was transformed into *E. coli* BL21 (DE3) host strain. (Cloning Primer Forward TAGACGCTAGCCATCATCACCATCACCCTCAGCCTCCAGCCGG; Cloning Primer Reverse GTTACCGTAAGCTTTTAGTGGCATCCACAAGCTC).

2.6. Site-directed mutagenesis

Human mature BMP6 sequence in pASK h-BMP6 plasmid underwent site-directed mutagenesis of the putative heparin/HS-binding domains (HBDS) of interest, aiming to substitute their clustered arginine and lysine residues with non-basic amino acids: R5L R6S R7L (HBD1), R39S K40N (HBD2) and K126N K127N R129S (HBD3). The substitutions were generated separately on different template pASK h-BMP6 plasmids, by Pfu polymerase PCR reaction (no. M7741, Promega) with the respective mutagenesis oligonucleotide primer pair, containing the desired mutations (Table 2). *DpnI* (Promega, cod. R6231) endonuclease selectively digested the methylated parental DNA template, allowing for mutated plasmids selection. The pASK h-BMP6 plasmids carrying concomitantly mutations on more than one HBD were generated by sequential mutagenesis reactions. The so obtained mutant plasmid constructs were verified by sequencing using Sanger method (Eurofins Genomics) and were used to transform *E. coli* BL21 (DE3) host strain for recombinant expression and solubilization of BMP6 mutants.

2.7. Expression of recombinant BMP6 wild-type and mutants in *E. coli* host strain

A suspension in Luria-Bertani (LB) broth (10 g/L Peptone, 5 g/L Yeast extract, 0.1 M NaCl, pH 7.4) of the pASK h-BMP6 transformed bacteria cells, was incubated overnight at 37 °C. Recombinant human BMP6 expression was induced by addition of 200 ng/mL of anhydrotetracycline (no. 2-0401-001, IBA) at 37 °C, under vigorous

agitation. After 4 h of induction bacteria cells were harvested by centrifugation, their pellet was resuspended in cold lysis buffer (0.1 M Tris-HCl pH 7.5, 1 mM EDTA, 1 mM PMSF) and then cell lysis was performed by sonication (Bandelin Ultrasonic Homogenizers HD 2070). The insoluble fraction was separated by centrifugation as a pellet. Insoluble bacteria inclusion bodies were washed with detergent-containing buffer (0.1 M Tris-HCl pH 7.5, 3% Triton-X 100) to remove bacteria cell debris. The inclusion bodies were solubilized by resuspension in 6 M Urea, 0.1 M DTT, 0.1 M Tris-HCl pH 7.5, 1 mM EDTA, followed by centrifugation to remove the still insoluble debris. The recombinant expression and solubilization of BMP6 mutants were performed using the same protocol.

2.8. Heparin-affinity chromatography

Solubilized inclusion bodies, containing BMP6 (wild-type and mutants), were analysed on HiTrap Heparin HP column (GE-Healthcare), connected to the Akta® prime FPLC system. The column was firstly equilibrated with the loading buffer (6 M urea, 5 mM DTT, 0.1 M Tris-HCl pH 7.5, 1 mM EDTA), then the solubilized inclusion bodies were loaded onto the column at a flow rate of 1 mL/min, while fractions were collected. An extensive washing step was performed with 20 column volumes of loading buffer, removing weakly heparin-bound proteins. Instead, the elution of heparin-binding proteins was achieved with NaCl gradient (Loading buffer +1 M NaCl). Absorbance at 280 nm and conductivity were recorded at column outlet and reported in a real-time chromatogram.

2.9. SDS-PAGE and immunoblotting

The proteins of chromatography fractions corresponding to column flow-through (washing step) and elution (NaCl gradient) were analysed by 15% SDS-PAGE in reducing conditions, staining with Coomassie Brilliant Blue R-250. For immunoblotting, after the electrophoresis the proteins were transferred to Hybond-P membrane (GE Healthcare Amersham). The saturation was performed in 2% defatted milk prepared in Tris-buffered saline buffer +0.05% tween20 (TBST). Incubation with primary antibody (α -6xHis mouse monoclonal antibody, Origene, cod. TA150088) and HRP-conjugated secondary antibody (HRP α -mouse antibody, BioFX Laboratories, cod. 11,012,102). The chemiluminescent signal was developed using SuperSignal West Femto Maximum Substrate (Thermo Scientific-Pierce) and acquired with LI-COR Odyssey® Fc imaging system.

2.10. Molecular mechanic and molecular dynamic simulation characterization

The heparin chain for the simulations (HEP) was modelled by an undecasaccharide GlcNS6S-(1-4)-IdoA2S-(1-4)-[GlcNS6S-(1-4)-IdoA2S]₄-GlcNS6S, where the monosaccharides GlcNS6S (N-sulfated-6-O-sulfated- α -D-glucosamine) and IdoA2S (2-O-sulfated- α -L-iduronic acid), representing an average heparin chain [14]. The conformations of the GlcNS6S and IdoA2S residues were set as ⁴C₁ and ¹C₄ chair respectively, as already established from heparin like oligosaccharides [19,20,24,41]. The IdoA2S conformation depend from the sulfation degree of the neighbouring residues. When IdoA2S is surrounded by two GlcNS6S its conformation appeared mixed by a nearly balanced contribution of two limit forms: the chair ¹C₄ and the skew boat ²S₀ [20]. Considering the experimental uncertainty in the fitting procedure of the NMR three bonds j-coupling constants (J_{HH}), in pure D₂O some authors observed that ¹C₄ weakly dominate the IdoA2S conformational equilibrium [19,20,27], while other researchers observed a weak prevalence of the ²S₀ [29]. In ionic strength condition nearer to physiological values, particularly in presence of Ca⁺² ions, the IdoA2S conformation further moves toward ¹C₄ until the percentage of these two ¹C₄/²S₀ reach values around 53/47% in a pentasaccharide, or 79/21% in heparin [20,31]. In

our classical Force Field model of heparin, the IdoA2S in a 'level zero' approximation was initially set to be purely ¹C₄, that even if it corresponds to the most populated limit conformation, is not unique, and for that reason it cannot fully describe the peculiar conformational features of this residue. The glycosidic dihedral angles (ϕ_1 -C1-O4-C4/C1-O4-C4-H4) of the HEP were set at the beginning as: ϕ_i/ψ_i -39/-33 and 41/14 degrees for the sequences: GlcNS6S-IdoA2S and IdoA2S-GlcNS6S respectively [24,41]. To describe the interaction between the BMP6 and heparin, models of the complex HEP-BMP6 were built manually approaching the HEP chain on the predicted heparin-binding domains (HDBs) on the 3D structure of the BMP6 monomer, obtained following the procedure in Fig. S1. The HEP-BMP6 complexes: HEP-BMP6 (HBD1), HEP-BMP6 (HBD2), HEP-BMP6 (HBD3) were built moving close the HEP (ligand) to each selected HBD until the shortest distances between the contacting surfaces reached values between 2.0 and 2.5 Å, and taking care to orient the approaching NS, 2O-S, 6O-S, sulfate clusters, that periodically decorate the external part of the heparin helix [22], toward the nearest HBD; this will allow the long-range electrostatic forces to drag the rest of the chain toward the HDB. A fourth complex HEP-BMP6 (HBD1/HBD3) was built adjusting the long enough HEP to contact both HBD1 and HBD3. The GLYCAM06 [34] and Amber [13] force fields were applied as HEP and BMP6 molecular mechanic parameters. MD simulation of approximate length of 320 ns in explicit solvent were run to optimize the geometry and the set of contacts of the HEP-BMP6 complexes (bound state), and that of HEP and BMP6 in unbound state as a comparison. All the MD simulation trajectories were sampled every 10 ps. The MD simulation cells were built surrounding each system by a 15 Å wide layer of water molecules (TIP3P) [32], generating a orthogonal box of hedge approximately 100 Å, where periodic boundary conditions were applied. The software Amertools 1.4 [12] and NAMD 12.2 [44] were used, the former to prepare the topology and geometry files, the latter to run the MD simulations. The equilibration period of the simulated HEP and HEP-BMP6 complexes were defined following two type of variables: the glycosidic dihedrals ϕ_i/ψ_i and the Root Mean Square Distance (RMSD) between the initial and the instantly evolving position of the HEP. The estimated binding energies, and their decomposition were calculated using the MMPBSA and MMGBSA methods (Molecular Mechanic Poisson Boltzmann Surface Area, and Molecular Mechanic Generalized Born Surface Area, Amber-tool 1.4). The three trajectories approach was applied, comparing the MD simulation trajectory of each of the tested complex HEP-BMP6 (230 to 310 ns, sample frequency of 80 ps) with the corresponding of HEP and BMP6 in unbound state. The ion concentration was set to 0.1 M, while no entropy contribution was included. In fact, the entropic term is considered comparable in each binding mode, where the same ligand HEP interact with different HBDs, the result is a 'consistent' scale of free energy of binding. Finally, this approach was also used to decompose the estimated energy of binding of each HEP-BMP6 complex, in the contribution that each residue of BMP6 apply.

2.11. CHO-K1 wild type and CHO mutant 745 cell monolayer binding assay

Wild-type Chinese Hamster Ovary (CHO-K1 ATCC® CCL-61) and mutant CHO-745 (pgsA-745 ATCC® CRL-2242 [16,17]) cells were maintained at 37 °C and 5% CO₂, in F12 medium (Euroclone) supplemented with 10% Fetal Bovine Serum (FBS, Euroclone), 40 µg/mL gentamicin sulfate (Euroclone), 2 mM l-glutamine (Euroclone) and 1 mM sodium pyruvate (Euroclone). Wild type and mutant CHO cells were seeded in a TC 96-well plate (Sarstedt) with a cellular density of 80.000 cells/well. Once the monolayers formed, the medium was removed, and cells were washed gently with PBS, fixed with 3% glutaraldehyde, incubating for 2 h at 4 °C, while the reaction was stopped adding glycine at a final concentration of 0.1 M. After PBS washing, the non-specific binding sites were saturated with PBS + 3% BSA. Synthetic BMP6 peptides (5, 25, 50, 250 µM in PBS + 3% BSA)

```

H. sapiens      SASSRRRQQSRNRSTQSQDVARVSSASDYNSSSEIKTACRKHELYVSFQDLGWQDWI IAPKGYAANYCDG
P. troglodytes SASSRRRQQSRNRSTQSQDVARVSSASDYNSSSEIKTACRKHELYVSFQDLGWQDWI IAPKGYAANYCDG
M. musculus    SASSRRRQQSRNRSTQSQDVSRGSGSSDYNGSEIKTACKKHELYVSFQDLGWQDWI IAPKGYAANYCDG
G. gallus      SAASRRRQQNRNRSTQAQDVSRVSTVTDYNSSDIKTACRKHELYVSFQDLGWQDWI IAPKGYAANYCDG
X. tropicalis  SATSKRKNQNRNRSTQAQDVSRVSSITDYNSSSEIKTACRKHELYVSFQDLGWQDWI IAPKGYAANYCGG
**:*:*:*:*:*:**:*:*:*:*:*:*:*:*:*:*:*:*:*:*:*:*:*:*:*:*:*:*:*:*:*:*:*:*
H. sapiens      ECSFPLNAHMNATNHAI VQTLVHLMNPEYVVPKPCCAPTKLNAISVLYFDDNSNVIIKKYRNMVVRACGCH
P. troglodytes  ECSFPLNAHMNATNHAI VQTLVHLMNPEYVVPKPCCAPTKLNAISVLYFDDNSNVIIKKYRNMVVRACGCH
M. Musculus    ECSFPLNAHMNATNHAI VQTLVHLMNPEYVVPKPCCAPTKLNAISVLYFDDNSNVIIKKYRNMVVRACGCH
G. gallus      ECSFPLNAHMNATNHAI VQTLVHLMNPDYVVPKPCCAPTKLNAISVLYFDDNSNVIIKKYRNMVVRACGCH
X. tropicalis  ECSFPLNAHMNATNHAI VQTLVHLMNPEYVVPKPCCAPTKLNAISVLYFDDNSNVIIKKYRNMVVRACGCH
*****:*:*:*:*:*:**:*:*:*:*:*:*:*:*:*:*:*:*:*:*:*:*:*

```

Fig. 1. Evolutionary amino acid sequence alignment of BMP6 mature fragment in different animal species. The protein alignment was performed with Clustal Omega software. Key symbols in protein alignment: (*) positions with a single fully conserved residue, (:) positions with conservation between amino acid groups of similar properties, (.) positions with conservation between amino acid groups of weakly similar properties. The lysine and arginine basic residues are in **bold**. Conserved basic residues clusters, representing potential heparin/HS-binding domains (HBDs), are framed in boxes.

were spotted onto cell monolayers and incubated 3 h at 37 °C. Unbound peptides were removed by washing with PBS, while cell-bound peptides were detected as previously described, taking advantage of their biotin tag.

2.12. Statistics

Data are shown as mean \pm SD. Statistical analysis was performed via ordinary One-way Anova or 2-way Anova (GraphPad Prism Software). Differences were considered as significant for p values <0.05 and represented as indicated in the figure's captions.

3. Results

3.1. Identification of heparin/HS-binding domains in the BMP6 sequence

The interaction of proteins with heparin/HS is mainly mediated by clusters of positive charged arginine and lysine residues that attract the negatively charged sulfate groups of heparin/HS [57]. In order to identify conserved basic residues cores, we aligned the mature BMP6 sequence from different animal species. Three conserved domains were identified, representing putative BMP6 heparin/HS-binding domains (HBDs) (Fig. 1).

These domains were localized near the N-terminus (HBD1), in central region (HBD2) and near the C-terminus (HBD3) (Fig. 1). The 3D structure of BMP6 (PDB ID: 2r52 [54]) showed that arginine and lysine residues of HBD2 and HBD3 were exposed and together generated a positively charged patch (Fig. 2). Since in the crystallographic structure of BMP6 the 1–34 N-terminal residues are unresolved, thus the conformation of HBD1 is unknown.

3.2. BMP6 synthetic peptides binding to solid-phase heparin

To validate if the identified domains (HBDs) bind heparin/HS, we firstly produced the corresponding synthetic peptides, covalently linked at N-terminal to a biotin tag, for detection in *in vitro* binding assays (Table 1). Their interaction with heparin was tested in a solid-phase system in which the binding occurs at solid-solution interface. Under these conditions, the Gibbs free energy of the interaction is composed by contributions of molecular recognition and of a surface work energy.

The interactions between heparin and the different BMP6 peptides were evaluated by in-plate colorimetric mass-based assay. In this assay we used heparin-coated plates, that were first validated with Fibroblast growth factor-2 (FGF-2), revealing a strong and saturable interaction, in good agreement with reported data [36] (Fig. S2). Then we analysed the

BMP6 peptides HBD1, HBD2 and HBD3 by spotting various concentrations of them (5, 25, 50, 250, 2500 nM) on the heparin-plates and incubating 18 h at 4 °C. Next, we added streptavidin-HRP conjugated and we developed the HRP activity. The N-terminal peptide (HBD1) and the C-terminal peptide (HBD3) exhibited saturable interaction that fitted the Langmuir model of adsorption for monovalent binding, allowing the calculation of their heparin-affinities, expressed as apparent dissociation constant (K_d') (Fig. 3A). HBD3 showed the highest affinity, ($K_d'_{HBD3} = 43.6 \pm 5.2$ nM), followed by HBD1 ($K_d'_{HBD1} = 216.4 \pm 38.7$ nM). HBD2 interaction was weaker and its K_d' could not be calculated. Next, we produced peptides in which the basic residues were substituted by non-charged ones in HBD1 (R5L, R6S, R7L) and in HBD3 (K126N, K127N, R129S) (Table 1). They were analysed in the solid-phase heparin assay, showing no detectable signal at any of the tested concentrations (Fig. 3A).

The HBD1 and HBD3 peptides were also tested by microcantilever (MC) biosensors operating in static mode, *i.e.* energy-based sensors [5]. The static mode operation of MCs exploits the fact that the biomolecular transformations occurring on one MC surface can cumulate and perform an overall surface work in the order of mJ m^{-2} [18]. An asymmetry between the upper and lower face of MC is needed in order to achieve a difference in the induced surface work on the two faces and generate deflection. The differential deflection is calculated subtracting the signal arising from the reference MCs (un-functionalized) from the signal of the functionalized MCs, preventing artifact deflections [2]. The Au face of the MCs was functionalized by selective adsorption of thiolated heparin, which was validated by antithrombin (AT) analysis. After injection of 1.5 μM AT, the heparin-functionalized MCs generated a differential deflection respect to the reference MCs of -26.0 ± 4.4 nm, thus reflecting a specific surface work driven by the interaction between AT and heparin molecules. Differential deflection of the MCs was also detected after injection of 25 μM of HBD1 or HBD3 peptides on the heparin-coating, while the respective mutants showed null or unspecific interaction (Fig. S3) at increasing concentrations (0.5, 5, 10, 25, 50 μM) for dose-response experiments. Data points were normalized and fitted with a Langmuir equation for monovalent binding, allowing to calculate an apparent equilibrium constant referred as nanomechanical surface equilibrium constant (K_d^σ) [39]. HBD1 and HBD3 peptides bound heparin with K_d^σ values of (6.0 ± 2.0) μM and (8.5 ± 1.0) μM , respectively (Fig. 3B), while the HBD2, HBD1 mutant and HBD3 mutant peptides showed no detectable interaction (not shown). The similarity of the two K_d^σ values (6.0 μM and 8.5 μM) indicates that the nanomechanical effect of the two peptides (such as conformational changes) on heparin is comparable. Moreover, the K_d^σ values fall in the range of μM , about two orders of magnitude higher than the apparent binding

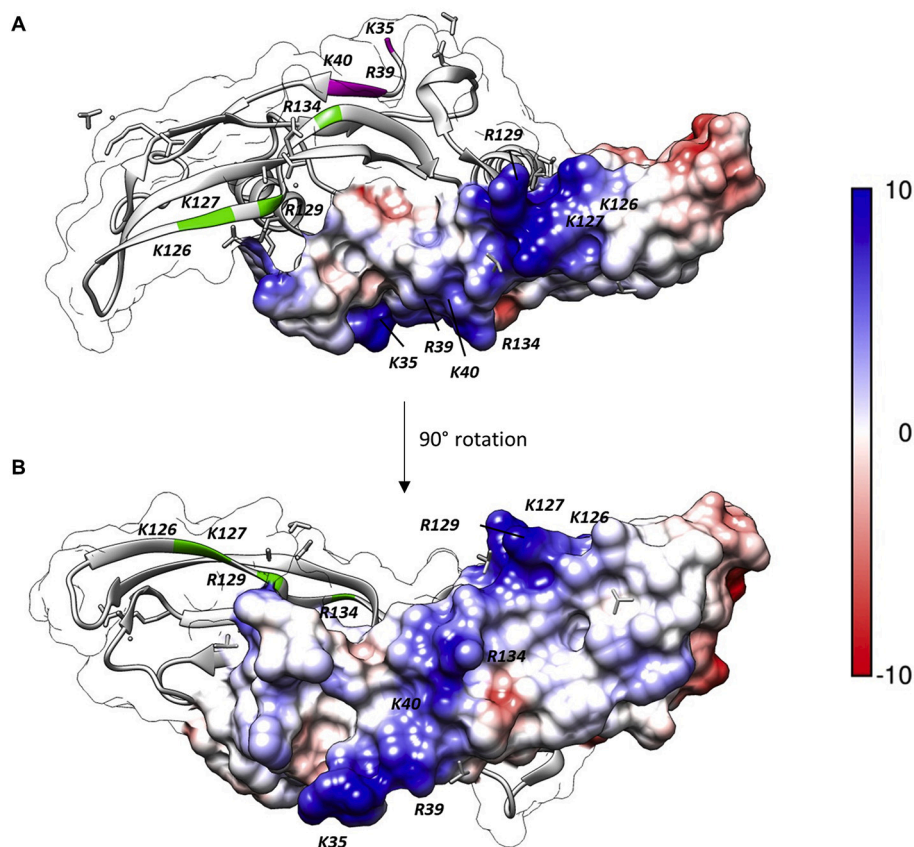


Fig. 2. BMP6 domains rich in basic residues. (A) Top and (B) front views of BMP6 dimer crystal structure (PDB ID: 2r52 [36]), lacking the highly unstructured N-terminus region [1,3,4,6–10,14,15,19,20,24–27,29,33,35,37,38,40–42,45–49,51,52,54,56,58], encompassing the HBD1 of interest. A BMP6 monomer was represented as cartoon, colouring basic residues in HBD2 (magenta) and HBD3 (green). The other monomer was coloured by electrostatic potential on the solvent accessible surface on a scale of -10 to $+10$ Kcal mol $^{-1}$ e $^{-1}$ (red to blue). The basic residues in putative HBDs were one-letter code labelled. This representation was generated using Chimera UCSF software.

affinity constants (K_d'), reflecting that in the studied interactions the surface work contribution is negligible with respect to the molecular recognition one. Altogether, the two assays indicated HBD1 and HBD3 to be the contact sites to heparin.

3.3. Glycosaminoglycans competition with BMP6-heparin binding

Basing on the knowledge that heparin/HS-binding proteins may be promiscuous for other GAGs, we designed a competition assay to study the BMP6 peptides specificity to heparin, compared to other GAGs. HBD1 or HBD3 peptides (50 nM) were pre-incubated with increasing concentrations of unfractionated heparin, chondroitin sulfate (CS) and dermatan sulfate (DS), prior to assay the binding on heparin-coated plates. HBD1 binding was competed off by unfractionated heparin in a dose-dependent manner, with a 20% decrease with 0.4 μ g/mL and 50–60% decrease with higher doses (1.2–3.6–11 μ g/mL), while CS and DS had only a minor effect, with a maximum reduction of 20% at the highest doses (Fig. 4A).

The HBD3 binding was competed off by heparin but also by DS (dose-dependent manner) and in a minor extent by CS, with a mean of 20% decrease of the signal (Fig. 4B). DS has a lower sulfation degree than heparin (average number of sulfates for disaccharide 1.1 versus 2.4) and the finding that DS competes with HBD3 but not with HBD1 suggests that in the second the electrostatic interactions are dominant, while in the former an additional contribution is possibly mediated by the hydrophobic amino acids M131; V132; V133. Basing on the finding that heparin sulfation degree influences its activity as hepcidin suppressor [46,47], we studied the competition also with partially desulfated heparins, expecting a diminished competition than unmodified heparin: Hep 2-O DeS and Hep 6-O DeS have lower sulfation degree in 2-O and 6-O positions, resulting in an average number of sulfates per disaccharide, respectively of 1.82 and 1.67, compared to 2.4 of unmodified heparin

(see methods section for details). Despite these partially desulfated heparins competed similarly to unmodified heparin (no significant difference), Fig. 4 qualitatively shows that the saturation behaviour of the competition grows with the degree of sulfation of the heparins. However, it is important to consider that these heparin preparations are only partially desulfated, thus residual sulfation on the heparin chain may still contribute to the peptides binding. The Fig. 4 provided only a qualitative picture of the sulfates role in BMP6-heparin interaction, while a description at molecular level remains to be determined.

3.4. Heparin-affinity chromatography of recombinant BMP6

We expressed the mature full-length recombinant human BMP6 in *E. coli* with a histidine (6xHis) tag linked at the N-terminus by cloning its cDNA into the anhydrotetracycline-inducible pASK-IBA43plus vector. The system produced large amounts of BMP6, which accumulated all in the insoluble fraction of the *E. coli* homogenates, and none in the soluble fraction. The BMP6 was solubilized in 6 M urea and reducing agents to study the heparin binding of the full-length protein using a heparin-affinity chromatography assay. The heparin column was equilibrated in 6 M urea, 5 mM DTT at pH 7.5, then the solubilized BMP6 was loaded and the eluted fractions collected. Most proteins were eluted in the flow-through and the heparin-bound proteins were eluted with a 0–1 M NaCl gradient, monitored by electric conductivity (Fig. 5A). SDS-PAGE analysis identified the BMP6 monomer of 15 kDa in the elution fractions (Fig. 5B), confirmed by immunoblotting with anti-6xHis antibody (Fig. 5C). BMP6 eluted from the heparin column at a conductivity of 19.82 mS cm $^{-1}$, corresponding to 0.35 M NaCl (dashed line in Fig. 5A).

3.5. Heparin-binding of recombinant BMP6 mutants

We produced various BMP6 mutants in which the basic residues of

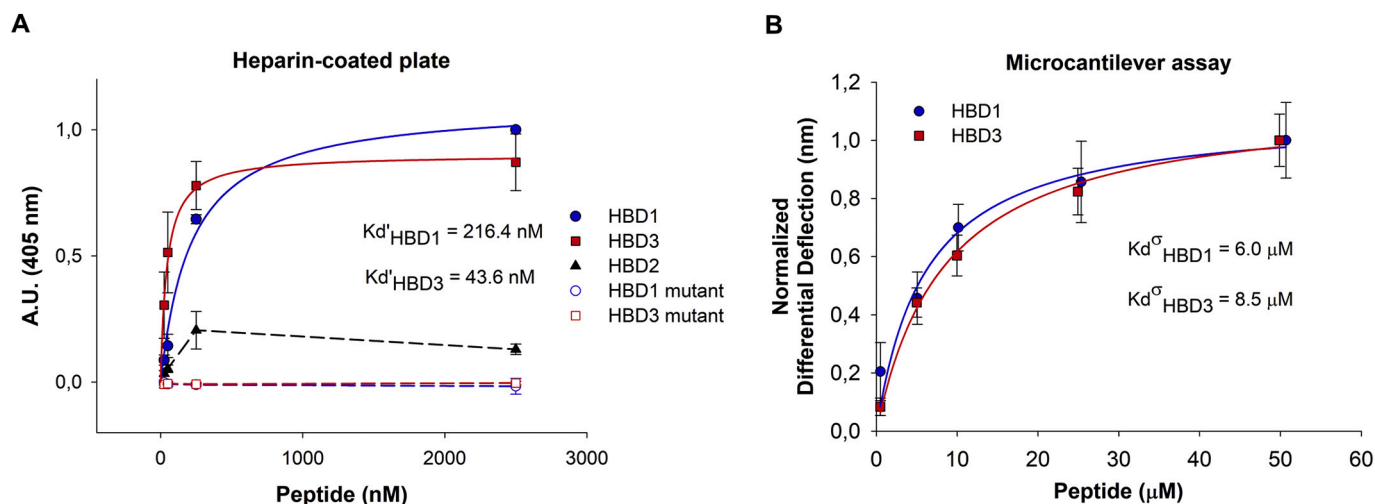


Fig. 3. BMP6 peptides binding to solid-phase heparin. (A) Heparin-coated plate were incubated with progressive concentrations (5, 25, 50, 250, 2500 nM) of HBD1 (blue circle), HBD3 (red square), HBD2 (black triangle), HBD1 mutant (empty blue circle) and HBD3 mutant (empty red square) biotinylated peptides. Binding was measured using streptavidin-HRP conjugated and TMB reactive, reading colorimetric signal at 405 nm. Binding isotherm of HBD1 and HBD3 (solid blue and red lines) was fitted to Langmuir equation. The HBD2 and mutant peptides did not fit the isotherm model (dashed black, blue and red lines). (B) Nanomechanical binding isotherm of HBD1 (blue circle) and HBD3 (red square) peptides tested at increasing concentrations (0.5, 5, 10, 25, 50 μM) on Microcantilevers functionalized with thiolated heparin. K_d , K_d^{σ} and the respective errors were calculated by the Langmuir fitting algorithm with 95% of confidence. Each marker represents mean value of at least three independent experiments and error bars indicates the standard deviation of the mean.

the three HBDs were substituted with neutral ones. They consisted in HBD1 mutant (R5L, R6S, R7L), HBD2 mutant (R39S K40N), HBD3 mutant (K126N, K127N, R129S) and the combined mutants HBD1 + 2 mutant, HBD1 + 3 mutant, HBD2 + 3 mutant, HBD1 + 2 + 3 mutant (listed in Tables 2 and 3).

They were all efficiently expressed in *E. coli*, solubilized as above and then loaded on the heparin column. The single mutants of HBD1 and HBD3 were retained by the heparin but eluted at a salt concentration lower than that of wild type BMP6 (elution peaks with conductivity of 9.88 mS cm^{-1} and 17.12 mS cm^{-1} , respectively versus 19.82 mS cm^{-1} of BMP6-wt). In turn, the HBD2 mutant eluted as BMP6 wt, and the addition of this mutation on the HBD1 and HBD3 mutants did not affect their elution points: the HBD2 mutant eluted at 19.60 mS cm^{-1} , the HBD1 + 2 mutant at 10.40 mS cm^{-1} and the HBD2 + 3 mutant at 18.67 mS cm^{-1} (Table 3).

More important, the combination of HBD1 and HBD3 mutations, in the HBD1 + 3 and HBD1 + 2 + 3 mutants, abolished BMP6 interaction with heparin, as they were found only in the flow through fractions by the SDS-PAGE analysis (Fig. 5D). We concluded that both N-terminal (HBD1) and C-terminal (HBD3) sites are involved in heparin binding, and they might co-operate in the binding long heparin chains.

3.6. Molecular modelling of the heparin-BMP6 interaction complex

Since the 3D structure of BMP6 (PDB ID: 2R52) [54] misses the N-terminal residues 1–34, a molecular dynamic (MD) approach was applied to predict its conformation (see procedure in Fig. S1). A frame after 39.07 ns of MD simulation in water solution was randomly extracted from a set of four, previously verified to have comparable random coil conformations (See Fig. S1). A secondary structure prediction method (GOR method [23]) was also applied confirming a prevalent random-coil conformation (Fig. S1). Its flexibility may facilitate protein adaptation to ligands, such as heparin. The BMP6-heparin interaction was then studied by MD simulations, useful to improve the “GAG-protein” docking, that involves electrostatic forces between long and flexible ligand-receptor [53]. This approach was firstly validated by simulating the well-characterized interaction between the pentasaccharide: GlcNS,6S-GlcA-GlcNS,3S,6S-IdoA2S-GlcNS,6S (AGA*IA) and the protein AT in explicit solvent condition until about 420 ns

(Fig. S4). The estimated Free Energy of binding was calculated with the “three trajectories” approach, that include the conformational changes upon binding of ligand and receptor, expressed as MMPBSA and MMGBSA [21]. Their respective values were -59 [58] and -50 [58] Kcal mol^{-1} in the AGA*IA-AT system, indicating a significant binding interaction [5]. Moreover, the binding energy per residue decomposition (Fig. S4 right) showed the favourable contribution of known key residues of AT in heparin binding (K11, R46, R47, K114, K125, R129) [30].

We then generated full-length BMP6 monomer to create binding models with a representative heparin chain (HEP) of 11 residues. The initial conditions were based on the identified BMP6 contact sites: HEP-BMP6 (HBD1), HEP-BMP6 (HBD2), HEP-BMP6 (HBD3), and HEP-BMP6 (HBD1/HBD3) (building details in material and method section). During the MD simulation the HEP chain is expected to be dragged by the long-range electrostatic forces between the positive patches on BMP6 and the negative sulfate clusters of heparin (GlcNS6S-IdoA2S-GlcNS6S) (Fig. S5) [22]. A manual docking followed by MD simulation in explicit solvent, was chosen instead of the automatic docking, that does not work properly with long oligosaccharide chain and with flexible active sites [11,43].

Therefore, the HEP-BMP6 complexes, and in parallel the HEP and BMP6 in unbound state, were submitted to MD simulation in explicit solvent for about 320 ns. RMSD function quantified the “distance” of the HEP chain position compared to the initial one: in HEP-BMP6 (HBD1), HEP-BMP6 (HBD2) and HEP-BMP6 (HBD3) the HEP position required at least 230 ns to equilibrate, while HEP-BMP6 (HBD1/HBD3) relaxed in 80–100 ns (Fig. S6). The conformational and contact analyses were performed comparing the equilibrated MD simulation trajectories of the HEP-BMP6 complexes to the HEP and BMP6 in unbound state (used as references). In Fig. 6 (upper section of each panel) the poses of each HEP-BMP6 complex, extracted from the equilibrated MD simulations, were reported as a qualitative molecular description of possible heparin-BMP6 arrangement into an interacting complex.

3.7. HEP-BMP6 binding energy estimation and contact analysis

We then estimated the free energy of binding (MMGBSA, MMPBSA) of each generated HEP-BMP6 complex (Fig. 6) paying attention to the

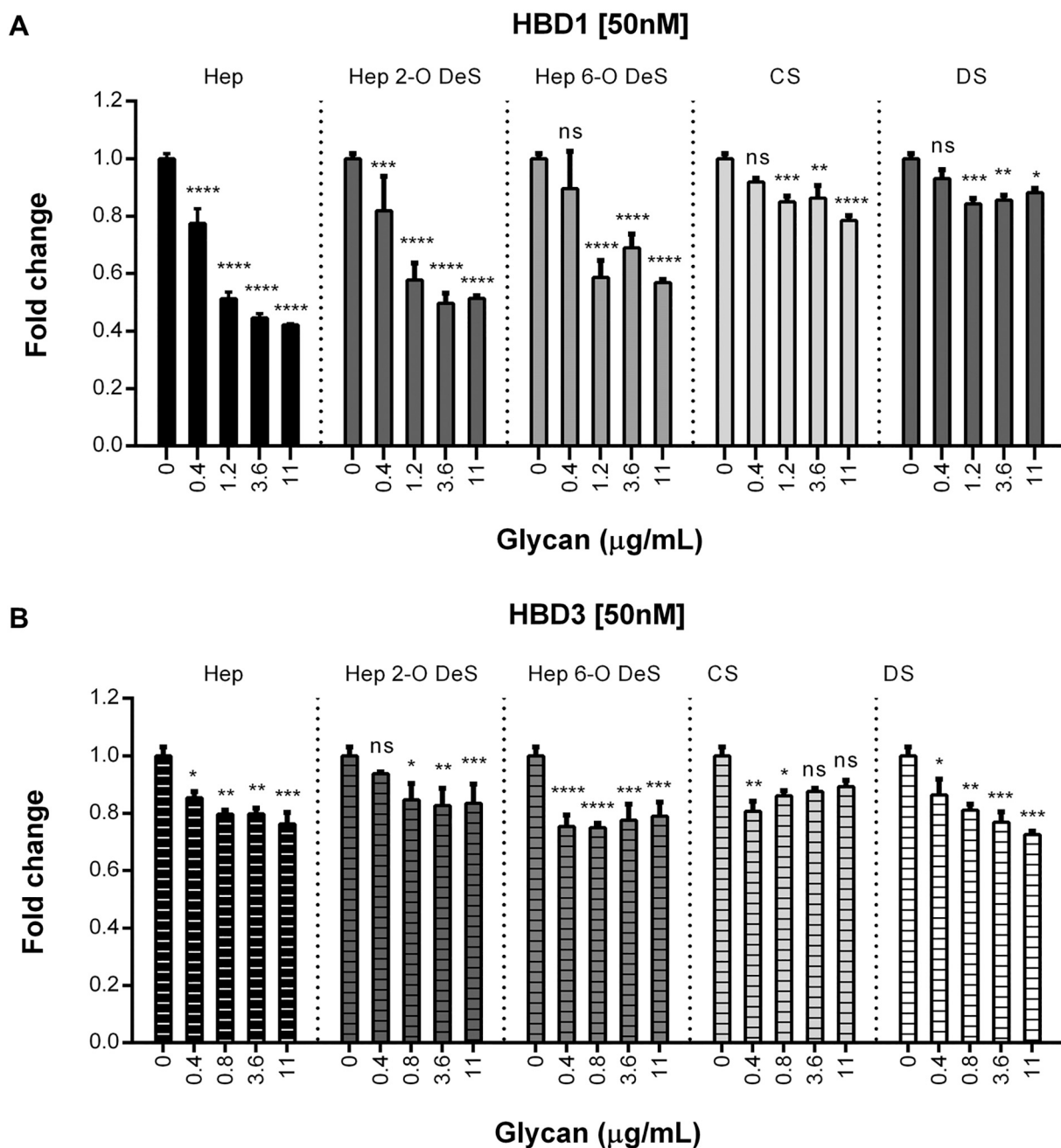


Fig. 4. BMP6 peptides heparin-binding competition assay with different glycans. A single dose (50 nM) of (A) HBD1 or (B) HBD3 biotinylated peptides was pre-incubated with different concentrations (0.4–1.2–3.6–11 $\mu\text{g}/\text{mL}$) of heparin (Hep), heparin 2-O desulfated (Hep 2-O DeS), heparin 6-O desulfated (Hep 6-O DeS), chondroitin sulfate (CS) or dermatan sulfate (DS). Binding was measured using streptavidin-HRP conjugated and TMB reactive, reading colorimetric signal at 405 nm. The values were normalized to the respective untreated peptide (0) and hence expressed as fold change. The graphs are means of three independent experiments. Differences among each experimental point and the respective untreated control were analysed by One-way Anova analysis with Graphpad Prism software (p values representation: **** $p \leq 0.0001$, *** $p \leq 0.001$, ** $p \leq 0.01$, * $p \leq 0.05$, ns non-significant).

ranking of the HBDs. The heparin complex with HBD3 and the HBD1/HBD3 sites were the most stable ones (Fig. 6C and D), in fact these sites are characterized by the lowest, and comparable binding energy values, followed by that of HBD1 (Fig. 6A). Differently, the HBD2 presents the weakest binding interaction (Fig. 6B). Interestingly, in this modelling description the heparin-BMP6 binding energy is comparable with that of heparin-AT (reference complex), while the ranking of the HBD sites in BMP6 is consistent with the *in vitro* results.

The binding energy decomposition shows the residues that contribute positively or negatively to the energy of binding and it was reported for each HEP-BMP6 complex (Fig. 6, lower section). The most

positively contributing amino acids were selected by - 4.0 Kcal mol^{-1} threshold, they were labelled in red on the histograms and drawn by yellow tubes. Notably, most of BMP6 residues with the strongest binding energy contribution, were comprised or adjacent to the HBDs of interest.

The HEP-BMP6 (HBD1) arrangement (Fig. 6A) showed that the residues R5, R7, V20 and V23 were those with the strongest energy contribution and closer contacts with HEP. A significant energy contribution was given by R13, D19, E33, R39 and V99, that were not in contact with the HEP. This correlates with the formation of two cluster of ion pairs R5, R13 vs D19, E33 and R39 vs D68, located in HBD1 and nearby to HBD2 respectively, whose flexible conformation would be in-

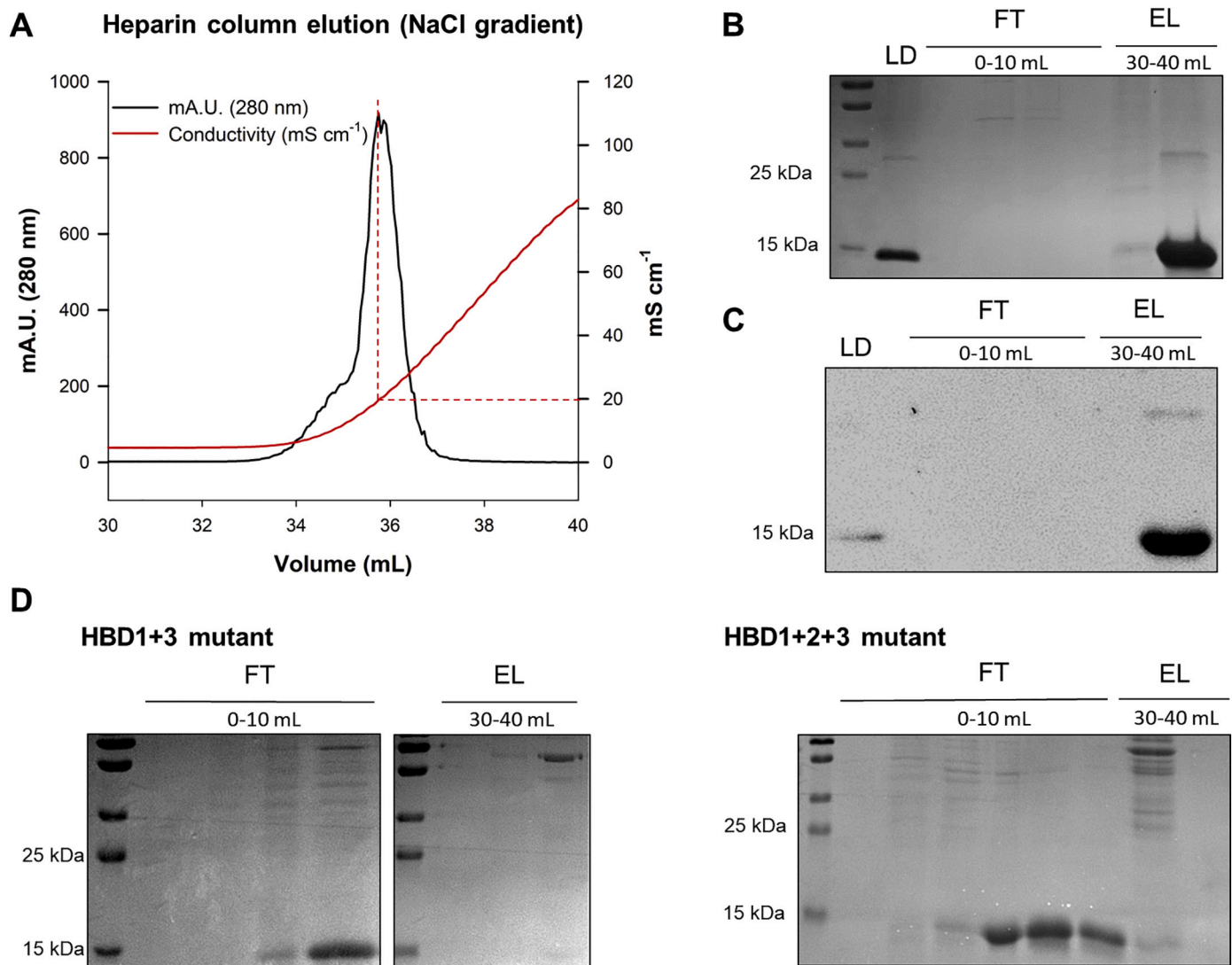


Fig. 5. Heparin-affinity chromatography (HAC) of recombinant BMP6 wild-type and mutants. (A) Chromatogram reporting the absorbance at 280 nm (black line) and conductivity (solid red line) during the elution of wild-type BMP6 from the heparin column. Conductivity at the elution peak is indicated with dashed red line. (B) Coomassie blue stained SDS-PAGE and (C) Immunoblot anti-6xHis tag of wild-type BMP6 fractions generated during HAC analysis. (D) SDS-PAGE of HAC fractions during HBD1 + 3 (left) and HBD1 + 2 + 3 (right) mutants BMP6 analysis, showing the presence of BMP6 only in the column flow-through, while it was absent in the elution fractions. (LD) column load, (FT) column flow-through fraction, (EL) elution fraction.

directly perturbed by the bound HEP. The HEP-BMP6 (HBD2) showed R13, R22, L34 and R39 with a significant binding energy contribution, with only the last two in close contact with HEP (Fig. 6B). The HEP-BMP6 (HBD3) complex (Fig. 6C) presented the HEP in contact with both the fingers and the wrist region of BMP6: K108, R129, K126, K127 and R134 belonging to HBD3 contributed significantly to the binding energy and were in contact with HEP. An additional HEP-BMP6 complex was generated to study a possible cooperative binding of HBD1 and HBD3 when interacting with a HEP chain longer than 6–8 residues. The flexibility of HBD1 was crucial for the formation of this complex HEP-BMP6 (HBD1/HBD3) to make multiple contacts (Fig. 6D). The histogram in Fig. 6D indicate that residues of HBD1 (R5, R6, R7, R11, R13, T15 and R22) and those of HBD3 (L115, L125, K127 and R134) contribute significantly to the energy of binding, even if only R6, T15, L115, L125, K127 and R134 were in contact with HEP.

Interestingly, two residues of HBD2 (T36, R39) contribute to the binding energy, although not in contact with HEP. Additional investigations will be required to establish whether BMP6 residues conformations were indirectly affected by the presence of HEP, during the binding, thus excluding their artificial contribution to the binding

Table 3

Heparin-affinity chromatography (HAC) analysis of BMP6 wild-type and mutants. Ionic strength required for wild-type and mutants BMP6 elution from the heparin-column is reported and expressed as conductivity (mS cm^{-1}), recorded at the elution peak. HBD1 + 3 and HBD1 + 2 + 3 BMP6 mutants did not bind the heparin-column; hence the respective conductivity parameter was not detected.

BMP6	Amino acid substitution	Conductivity at elution peak (mS cm^{-1})
Wild type	–	19.82
HBD1	R5L R6S R7L	9.88
HBD2	R39S K40N	19.60
HBD3	K126N K127N R129S	17.12
HBD1 + 2	R5L R6S R7L R39S K40N	10.40
HBD1 + 3	R5L R6S R7L K126N K127N R129S	–
HBD2 + 3	R39S K40N K126N K127N R129S	18.67
HBD1 + 2 + 3	R5L R6S R7L R39S K40N K126N K127N R129S	–

energy. This could be the case of V99 which contribution to the binding energy was always found, even if V99 is far from each HBDs and HBD1/HBD2 flexible region. This analysis confirmed that HEP chain applies as favourite contacts the clusters of sulfates (GlcNS6S-IdoA2S-GlcNS6S) in every HEP-BMP6 complex (Table S1 and Fig. S5).

3.8. HEP conformational changes upon-binding

The conformations of HEP in the HEP-BMP6 complexes were compared with the ones of unbound state, using MD simulations of similar length and equilibration history. In this description, the GlcNS6S residues maintained their 4C_1 conformation in all the complexes (bound state) and in unbound state, as observed in heparin [19,28]. The modelled IdoA2S residues qualitatively mimicked the conformational flexibility observed in heparin, that is correlated to the sulfation degree of the neighbouring GlcN [19,20]. In particular, IdoA2S surrounded by two GlcNS6S, in heparin chains and oligosaccharides presents a mixed conformation in which the 1C_4 and 2S_0 contributions nearly balance, when the environment has a low ionic strength (See Materials and Methods). In IdoA2S the key distance ratio approximately: H2-H5/H4-H5 = 4.0/2.4 corresponds to a pure 1C_4 , while values near to 1.0 indicate a pure 2S_0 . Table 4 showed that either in unbound HEP and in bound states with BMP6 using HBD1 or HBD2, the conformation of IdoA2S were in 1C_4 . While, when the HEP bound HBD1/HBD3 four out of five IdoA2S were in 1C_4 , while the fifth presented a distorted 1C_4 . Differently, the HEP in bound state with HBD3 showed two IdoA2S residues with a 2S_0 , (H2-H5/H4-H5 = 2.5/2.3) and one with a distorted 1C_4 conformation (H2-H5/H4-H5 = 3.5/2.5). Then, HBD3 alone or in combination with HBD1 showed greater tendency to induce conformational changes on IdoA2S residues of HEP, reflecting the observed energy contribution in HEP binding.

The HBDs propensity to induce a glycosidic backbone conformational change on HEP upon binding was quantified by the number of glycosidic dihedral ($\Delta\phi_i/\Delta\psi_i$) with variation greater than 10° (Fig. S7). This backbone conformational change upon binding, similarly, as observed for IdoA2S, qualitatively describe the ability of the ligand (HEP) "to adapt" itself to the HBD surface establishing the contacts and it is proportional to the binding energy. However, the different flexibility of the HBDs should be considered as well. In fact, a less structured domain of BMP6 like HBD1, could adapt itself to the ligand, leaving the latter unchanged, as reflected by our HEP-change prediction studies. Consistent with these observations, the predicted scale of glycosidic backbone conformational change: HBD3 > HBD1/HBD3, HBD2 > HBD1 is found in partial agreement with the scale of binding energy reported in Fig. 6. More interestingly, these predicted conformational change of HEP could be considered as markers for selected HEP-BMP6 interactions.

3.9. BMP6 peptides interaction with cell membrane-HS

Natural heparin chains have lower molecular weight and higher degree of sulfation compared to the cell membrane proteoglycan HS chains [50]; for that reason HS interaction with BMP6 could not be exhaustively modelled by heparin. To investigate the binding properties of BMP6 peptides and recombinant protein to cell membrane-bound HS chains we prepared homogeneous monolayers of CHO-K1 cells. They have been extensively characterized for membrane-associated HS chain expression [17] and as negative control we used the GAGs-deficient mutant cell line CHO-745 [16], that allows to discriminate for HS-specific binding. Different doses of BMP6 peptides (5, 25, 50, 250 nM) were used to study their binding to membrane HS of CHO-K1 cells, in comparison with that to HS-free CHO-745 cell monolayer. HBD1 peptide showed the strongest dose-dependent binding to the cells expressing HS, and the signal was significantly higher than that obtained with the HS-deficient cell monolayers, at the doses of 50 and 250 nM (Fig. 7A). As expected, HBD2 peptide did not give HS-binding signal (Fig. 7B). HBD3

peptide showed a dose-dependent interaction with HS, and a preferential interaction with HS-expressing cells was evident only at the highest dose tested (250 nM) (Fig. 7C). The same approach was used to analyse the recombinant BMP6 binding to the cells. It showed a stronger signal with CHO-K1 than with CHO-745 monolayer, in a dose-dependent manner, suggesting that also the full-length protein can interact with membrane-bound HS (Fig. S8). Altogether these data confirmed the importance of the HBD1 and HBD3 sites for binding to membrane HS and heparin, although the order of affinity seems to be opposite for the two: HBD1 is higher for HS and HBD3 is higher for heparin. This discrepancy might be due to the different composition of the membrane HS compared to a porcine mucosa heparin.

4. Conclusions

The BMP6 interaction with heparin and HS was initially suggested by the observations that exogenous heparin inhibits the BMP6-induced hepcidin expression, while hepatic HS facilitate BMP6 activity [3,45–49]. However, a biochemical characterization of BMP6 interaction with this family of sulfated glycans was missing until recently, when Billings et al. in 2018 using various peptides showed that BMP6 binds HS with high affinity with a domain at C-terminus, differently by BMP2/4 that have one binding domain at the N-terminus (Fig. S9) [6]. The presence of a C-terminal heparin/HS-binding domain (HBD) in BMP6 is in agreement with our observation that the activity of the commercial recombinant BMP6s is strongly inhibited by heparin even though they are truncated at the N-terminus [3,45–48].

In this work we investigated BMP6 interaction with heparin and HS identifying three arginine- and lysine-rich clusters as putative HBDs. The study of the corresponding synthetic peptides in heparin binding led us to similar conclusions to those of Billings et al. [6], in which the major heparin-interacting peptide is proximal to the BMP6 C-terminus (involving K126, K127 and R129) (HBD3). However, we found that also basic cluster at N-terminus of BMP6 (carrying R5, R6 and R7) (HBD1) represents an additional putative binding site.

The specificity of the BMP6 peptide-heparin interactions was analysed by different approaches. Firstly, we dissected the molecular recognition and the surface work components of peptide-heparin binding energy at solid phase, taking advantage of heparin-functionalized plates and MCs, respectively. Both approaches demonstrated HBD1 and HBD3 peptides binding to heparin, however the surface work, which drives conformational changes, revealed to be negligible compared to the molecular recognition, as they generated apparent affinity constants in the range of μM and nM, respectively.

Next, the substitution of the clustered basic residues with non-charged ones (R5L R6S R7L on HBD1; K126N K127N R129S on HBD3), completely abolished the heparin-binding activities of the peptides. Intriguingly, some properties of the two sites differed, since HBD1 peptide interaction with heparin was competed off only by pre-incubation with heparin, while HBD3 interaction was competed off also by the less sulfated GAGs, DS. Therefore, this result suggests that the specificity of the HBD1 peptide in selecting the highly sulfated heparin, is likely correlated to a driving electrostatic interaction among basic residues and the sulfate groups. Instead, the promiscuous GAGs-binding activity of the HBD3 peptide is probably due to an additional hydrophobic contribution, suggested by the hydrophobic amino acids (M131; V132; V133) present in HBD3 and absent in HBD1, that may apply favourable contacts with the less polar DS.

Basing on the knowledge that heparin potency as hepcidin repressor increases with the degree of sulfation [46,47], we studied the peptide-heparin competition abilities of Hep 2-O DeS and Hep 6-O DeS, heparins that were partially desulfated in 2-O and 6-O positions, respectively. However, we found that both the modified heparins competed with the heparin-peptides interactions slightly less or similarly to unmodified heparin. Considering that these heparin preparations are only partially desulfated, we cannot exclude that residual sulfates on the heparin chain

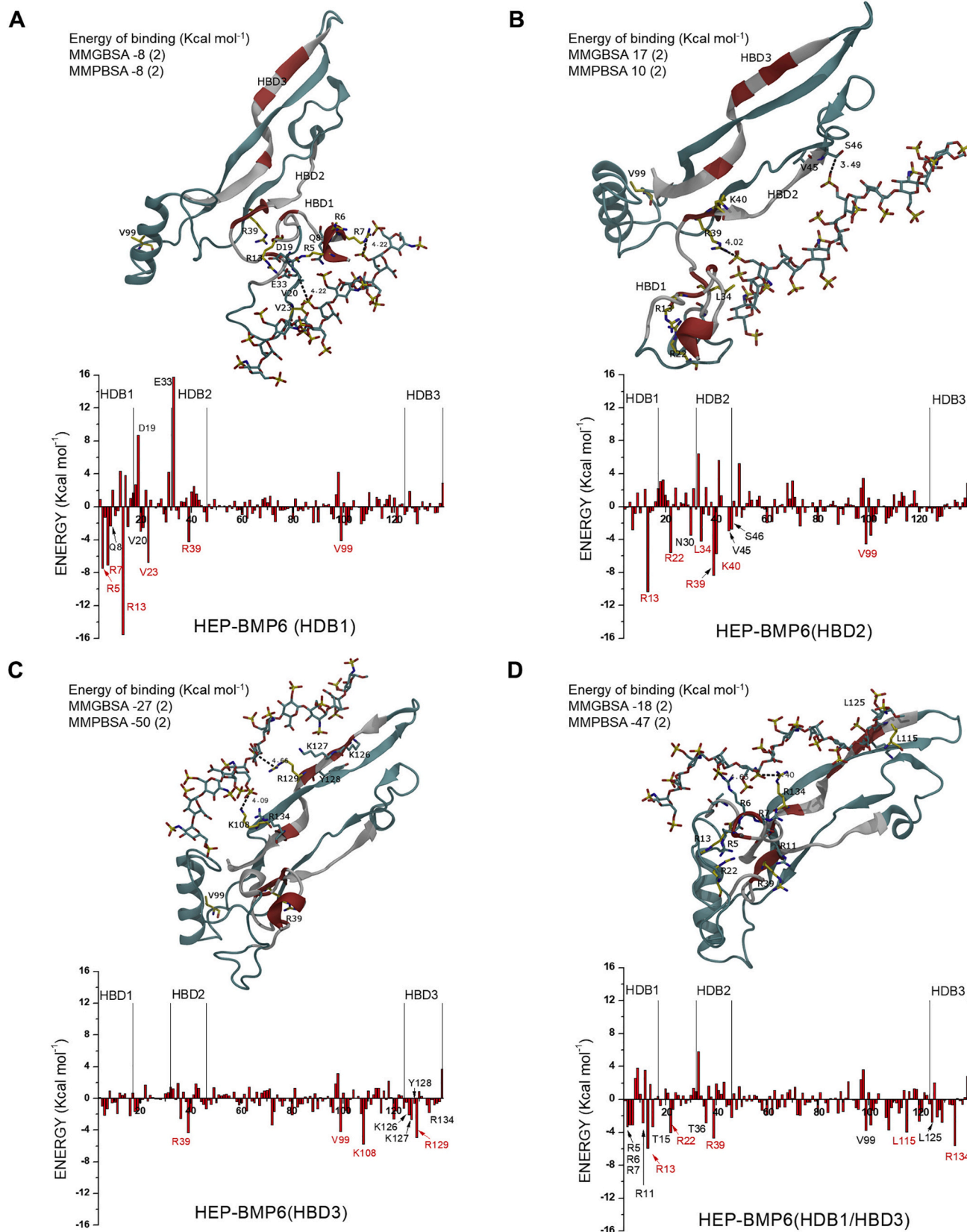


Fig. 6. HEP-BMP6 complex structures predicted by molecular dynamics. The top section of each panel shows the complex geometries generated by MD simulation (simulation time 310 ns) and the respective values of the estimated energy of binding, calculated from the equilibrated MD simulation trajectory (from 230 to 310 ns) using the MMGBSA and MMPBSA approximations. The corresponding energy of binding decomposition histogram is reported in the bottom section of each panel. Residues of both HBD3 and HBD1 domains that show the strongest contribution to the energy of binding (< -4.0 Kcal mol⁻¹) are underlined as yellow tubes on the complex structures, and as red labels on the histograms. Additional neighbour residues of BMP6 involved in HEP-BMP6 contacts are reported in cyan tubes on the structure complex, and as black labels on the histograms.

Table 4

HEP conformational changes upon-binding Average H2-H5 and H4-H5 distances of IdoA2S residue calculated on the equilibrated MD simulation (230 and 310 ns) for the HEP in un-bound state (HEP, first row) and in bound state with BMP6, according to the selected binding epitopes (second to fifth rows). IdoA2S residues from the Non-reducing to the reducing end are reported in column from 2nd to 6th. Bold face and underlined characters correspond to ratios indicating the 2S_0 skew boat conformation and a distorted 1C_4 . Distances are in Å, estimated Error on the mean are smaller than 0.1 Å.

	I2S (12) H2H5/ H4H5	I2S (11) H2H5/ H4H5	I2S (10) H2H5/ H4H5	I2S (9) H2H5/ H4H5	I2S (8) H2H5/ H4H5
HEP	4.0/2.4	4.0/2.4	4.0/2.4	3.8/2.5	3.9/2.4
HEP-BMP6 (HBD1)	4.0/2.4	4.0/2.4	3.9/2.4	3.9/2.4	3.9/2.4
HEP-BMP6 (HBD2)	4.0/2.4	3.9/2.4	3.9/2.4	3.9/2.4	3.9/2.4
HEP-BMP6 (HBD3)	<u>3.5/2.5</u>	4.0/2.4	2.5/2.3	2.5/2.3	3.8/2.4
HEP-BMP6 (HBD1/ HBD3)	3.9/2.4	4.0/2.4	4.0/2.4	3.9/2.4	<u>3.4/2.4</u>

were still enough to compensate the diminished sulfation in 2-O and 6-O positions. We concluded that even though our previous works suggested a clear dependence on the sulfation levels of heparin biological activity in terms of hepcidin repression, we could not rule out a clear dependence on sulfates of BMP6-peptides-heparin interaction, through the proposed assay. In fact, purposely designed experiments should be performed to dissect the molecular contribution of sulfates in BMP6-heparin interaction, a field of research that remains open to investigation.

The role of the identified HBDs was then investigated with the full-length BMP6 produced in *E. coli*, which was insoluble and thus needed to be solubilized, as reported by other investigators [54]. We tried to re-fold the solubilized protein *in vitro*, adapting a renaturation procedure reported for BMP2 [55]. This challenging procedure led to protein aggregation and consequent precipitation, limiting the yield of dimeric BMP6 and thus making impossible the characterization of its heparin/HS interactions. However, the recombinant BMP6 monomer showed affinity binding to the heparin-column that was diminished by substituting the basic residues with non-charged ones on HBD1 or HBD3 and completely abolished by concomitant mutation on both domains. This result also suggested the possibility of co-operation between the BMP6 C-terminal and N-terminal sites in binding long heparin/HS chains, *i.e.* bridging these sites.

All our multiple efforts to produce the dimeric mature BMP6 in

mammalian cells led again to insoluble proteins, possibly because the N-terminal extension interferes with the folding, a fact that would explain why the commercial ones lack of it. The expression in an eukaryotic system would also have allowed to study the effect of protein glycosylation, that was reported to influence BMP6 interaction with ALK2 type I BMP receptor [54]. It remains to be clarified whether glycosylation affects BMP6 binding to other molecules.

We also applied molecular dynamic simulations to study the heparin-BMP6 complex. To this aim, we firstly modelled the conformation of the N-terminal portion (residues 1–34) that contains the HBD1, but is missing in the crystallographic structure of BMP6 (PDB ID: 2R52) [54], that revealed to be a highly flexible random coiled structure that may allow the protein adaptation to the ligand. Then we used the so-obtained complete 3D structure of BMP6 monomer to model the interaction with a representative heparin chain (HEP) by MD simulations in explicit solvent. The most stable complexes were formed using HBD3 and HBD1 as contact sites, exclusively or concomitantly analysed. Moreover, the binding energy decomposition showed that the most residues directly or indirectly favouring the interaction, corresponded to the previously identified basic residues cores (R5 R6 R7 and K126 K127 R129), confirming the *in vitro* observations. We also observed that the HEP chain underwent conformational changes occurring upon binding HBD3, alone or together with HBD1, but not when binding to HBD1 alone, consistently with the predicated high flexibility of HBD1. This was also reflected during the concomitant interaction with HBD1 and HBD3, that showed HBD1 bending toward HBD3, hence supporting a co-operative behaviour.

In addition, we studied the binding to the HS on cell membrane, that are not structurally identical to heparin [50] and we confirmed that they are bound by HBD1 peptide, HBD3 peptide and the recombinant BMP6 monomer.

In conclusion, the *in vitro* and *in silico* approaches in this study are consistent and show that BMP6 N-terminal R5, R6 and R7 and C-terminal K126, K127 and R129 clusters are crucial for the heparin/HS-interaction. Our results also suggest the possibility of a cooperative activity of these domains during the formation of heparin/HS-BMP6 binding complex, with different roles: C-terminal HBD3 as the major contributor to the binding energy and N-terminal HBD1 endowed with flexible adaptation to the ligand.

Altogether, this study supports the model that was proposed before: HS acts as BMP6 co-receptor on the hepatocytes to sustain the BMP/SMAD signalling, conversely exogenous heparin sequesters BMP6 and inhibits the signalling, similarly to an R-decoy mechanism. Of interest is the presence of two binding domains located in opposite sides of BMP6 molecule, in contrast with other BMPs that typically have only one site.

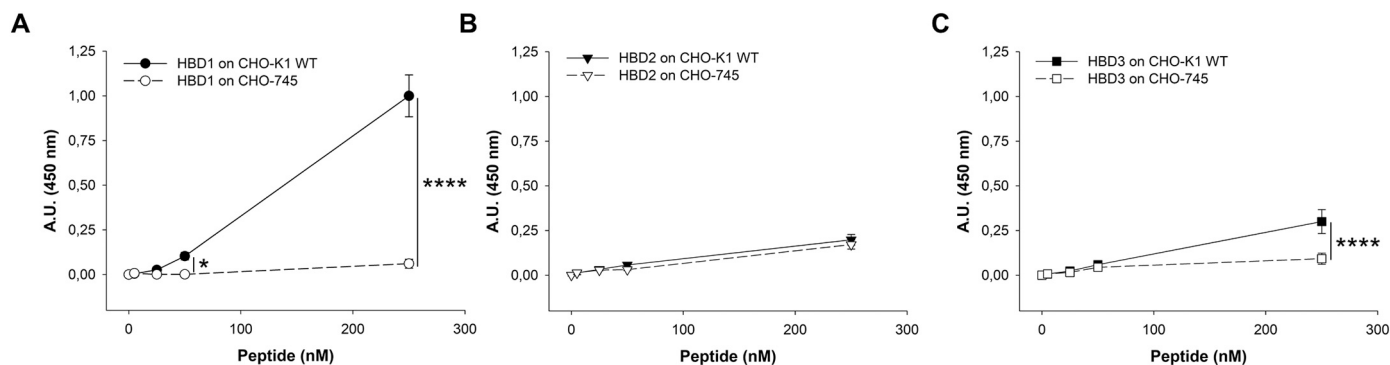


Fig. 7. BMP6 peptides interaction with cell-expressed membrane HS. The CHO-K1 WT and 745 cell lines were utilized to generate fixed cell monolayer to assess BMP6 peptide HS-binding activity. (A) The N-terminal HBD1 peptide, (B) the central HBD2 peptide and (C) the C-terminal HBD3 peptide interaction with CHO-K1 WT (black circle, triangle or square) and CHO-745 (white circle, triangle or square) monolayers was evaluated. Binding was measured using streptavidin-HRP conjugated and TMB reactive, reading colorimetric signal at 405 nm. The values resulting from three independent experiments were reported in plot. Differences among each experimental point and the respective control were analysed for their statistical significance by 2-way Anova analysis with Graphpad Prism software (*p* values representation: **** $p \leq 0.0001$, * $p \leq 0.05$, non-significant where no-symbol is reported).

The cooperativity of these domains in binding heparin may reflect that heparin/HS binding is more important for BMP6 than for other BMPs. This would partially explain why one of the major phenotypes of mice with diminished liver-specific HS sulfation was a reduction of hepcidin expression [4]. Eventually, it is also known that BMP6 shares some homology with the other components of its BMP subfamily, such as BMP5, BMP7 and BMP8. It means that also these BMP6 homologous could interact with heparin and HS through the same two sites.

Authorship

A.D.: designed research, performed research, analysed data and wrote the paper;

SE.: performed the *in-silico* studies and contributed to write the paper;

S.F.: performed the Microcantilever studies and revised the paper;

M.A., M.G., P.R., F.C.: performed research and revised the paper;

P.A.: contributed to design of research and revised the paper.

P.B., A.N: revised the paper.

M.P.: designed research, analysed data and wrote the paper.

Declaration of Competing Interest

The authors declare no competing financial interests.

Acknowledgements

We are grateful to Dr. Emiliano Esposito from G. Ronzoni Institute, Milan for the preparation of thiolated heparin. The work was partially supported by M.P. with ex60% from the University of Brescia, Brescia. The funders had no role in study design, data collection and analysis, decision to publish, or preparation of the manuscript. The work of S. E. was supported by G. Ronzoni Institute, Milan.

Appendix A. Supplementary data

Supplementary data to this article can be found online at <https://doi.org/10.1016/j.bbagen.2020.129799>.

References

- [1] B. Andriopoulos, E. Corradini, Y. Xia, S.A. Faasse, S. Chen, L. Grgurevic, et al., BMP6 is a key endogenous regulator of hepcidin expression and iron metabolism, *Nat. Genet.* 41 (4) (2009) 482–487.
- [2] J.L. Arlett, E.B. Myers, M.L. Roukes, Comparative advantages of mechanical biosensors, *Nat. Nanotechnol.* 6 (4) (2011) 203.
- [3] M. Asperti, A. Naggi, E. Esposito, P. Ruzzenenti, M. Di Somma, M. Gryzik, et al., High sulfation and a high molecular weight are important for anti-hepcidin activity of heparin, *Front. Pharmacol.* 6 (2016) 316.
- [4] M. Asperti, T. Stuemler, M. Poli, M. Gryzik, L. Lifshitz, E.G. Meyron-Holtz, et al., Heparanase overexpression reduces hepcidin expression, affects iron homeostasis and alters the response to inflammation, *PLoS One* 11 (10) (2016), e0164183.
- [5] P. Bergese, M. Cretich, C. Oldani, G. Oliviero, G. Di Carlo, L. Depero, et al., Advances in parallel screening of drug candidates, *Curr. Med. Chem.* 15 (17) (2008) 1706–1719.
- [6] P.C. Billings, E. Yang, C. Mundy, M. Pacifici, Domains with highest heparan sulfate-binding affinity reside at opposite ends in BMP2/4 versus BMP5/6/7: implications for function, *J. Biol. Chem.* 293 (37) (2018) 14371–14383.
- [7] J.R. Bishop, M. Schuksz, J.D. Esko, Heparan sulphate proteoglycans fine-tune mammalian physiology, *Nature*. 446 (7139) (2007) 1030–1037.
- [8] B. Bragdon, O. Moseychuk, S. Saldanha, D. King, J. Julian, A. Nohe, Bone morphogenetic proteins: a critical review, *Cell. Signal.* 23 (4) (2011) 609–620.
- [9] J. Brkljacic, M. Pauk, I. Erjavec, A. Cipic, L. Grgurevic, R. Zadro, et al., Exogenous heparin binds and inhibits bone morphogenetic protein 6 biological activity, *Int. Orthop.* 37 (3) (2013) 529–541.
- [10] S. Canali, K.B. Zumbrennen-Bullough, A.B. Core, C.-Y. Wang, M. Nairz, R. Bouley, et al., Endothelial cells produce bone morphogenetic protein 6 required for iron homeostasis in mice, *Blood*. 129 (4) (2017) 405–414.
- [11] A.D. Cardin, H.J.R. Weintraub, Molecular modeling of protein-glycosaminoglycan interactions, *Arteriosclerosis* 9 (1) (1989) 21–32.
- [12] D.A. Case, T.A. Darden, T.E. Cheatham, C.L. Simmerling, J. Wang, R.E. Duke, et al., AMBER 11, University of California, San Francisco, 2010.
- [13] D. Case, T. Darden, C. Simmerling, T.E. Cheatham III, K. Merz, Amber11 User's Manual. Amber, 2011.
- [14] B. Casu, Structure of heparin and heparin fragments, *Ann. N. Y. Acad. Sci.* 556 (1989) 1–17.
- [15] J.D. Esko, S.B. Selleck, Order out of Chaos: assembly of ligand binding sites in Heparan sulfate, *Annu. Rev. Biochem.* 71 (2002) 435–471.
- [16] J.D. Esko, T.E. Stewart, W.H. Taylor, Animal cell mutants defective in glycosaminoglycan biosynthesis, *Proc. Natl. Acad. Sci.* 82 (10) (1985) 3197–3201.
- [17] J.D. Esko, A. Elgavish, T. Prasthofer, W.H. Taylor, J.L. Weinke, Sulfate transport-deficient mutants of Chinese hamster ovary cells. Sulfation of glycosaminoglycans dependent on cysteine, *J. Biol. Chem.* 261 (33) (1986) 15725–15733.
- [18] S. Federici, G. Oliviero, D. Maiolo, L.E. Depero, I. Colombo, P. Bergese, On the thermodynamics of biomolecule surface transformations, *J. Colloid Interface Sci.* 375 (1) (2012) 1–11.
- [19] D.R. Ferro, A. Provasoli, M. Ragazzi, G. Torri, B. Casu, G. Gatti, et al., Evidence for conformational equilibrium of the sulfated L-Iduronate residue in heparin and in synthetic heparin mono- and oligosaccharides: NMR and force-field studies, *J. Am. Chem. Soc.* 108 (21) (1986) 6773–6778.
- [20] D.R. Ferro, A. Provasoli, M. Ragazzi, B. Casu, G. Torri, V. Bossennec, et al., Conformer populations of l-iduronic acid residues in glycosaminoglycan sequences, *Carbohydr. Res.* 195 (2) (1990) 157–167.
- [21] S.I. Fujiwara, T. Amisaki, Identification of high affinity fatty acid binding sites on human serum albumin by MM-PBSA method, *Biophys. J.* 94 (1) (2008) 95–103.
- [22] H.G. Garg, R.J. Linhardt, C.A. Hales, Chemistry and Biology of Heparin and Heparan Sulfate. Chemistry and Biology of Heparin and Heparan Sulfate, 2005, pp. 1–28.
- [23] J. Garnier, J.-F. Gibrat, B. Robson, [32] GOR method for predicting protein secondary structure from amino acid sequence, in: *Methods in Enzymology*, 1996, pp. 540–553.
- [24] M. Guerrini, S. Guglieri, B. Casu, G. Torri, P. Mourier, C. Boudier, et al., Antithrombin-binding octasaccharides and role of extensions of the active pentasaccharide sequence in the specificity and strength of interaction: evidence for very high affinity induced by an unusual glucuronic acid residue, *J. Biol. Chem.* 283 (39) (2008) 26662–26675.
- [25] C.A. Harrison, S.L. Al-Musawi, K.L. Walton, Prodomains regulate the synthesis, extracellular localisation and activity of TGF- β superfamily ligands, *Growth Factors* 29 (5) (2011) 174–186.
- [26] C.H. Heldin, A. Moustakas, Role of Smads in TGF β signaling, *Cell Tissue Res.* 347 (1) (2012) 21–36.
- [27] M. Hricovini, M. Hricovini, Solution conformation of heparin tetrasaccharide. DFT analysis of structure and spin-spin coupling constants, *Molecules* 23 (11) (2018) 3042.
- [28] M. Hricovini, M. Guerrini, A. Bisio, G. Torri, M. Petitou, B. Casu, Conformation of heparin pentasaccharide bound to antithrombin III, *Biochem. J.* 359 (Pt2) (2001) 265–272.
- [29] P.H. Hsieh, D.F. Thieker, M. Guerrini, R.J. Woods, J. Liu, Uncovering the relationship between sulphation patterns and conformation of iduronic acid in heparan sulphate, *Sci. Rep.* 6 (2016) 29602.
- [30] L. Jin, J.P. Abrahams, R. Skinner, M. Petitou, R.N. Pike, R.W. Carrell, The anticoagulant activation of antithrombin by heparin, *Proc. Natl. Acad. Sci. U. S. A.* 94 (26) (1997) 14683–14688.
- [31] L. Jin, M. Hricovini, J.A. Deakin, M. Lyon, D. Uhrin, Residual dipolar coupling investigation of a heparin tetrasaccharide confirms the limited effect of flexibility of the iduronic acid on the molecular shape of heparin, *Glycobiology* 19 (2009) 1185–1196.
- [32] W.L. Jorgensen, J. Chandrasekhar, J.D. Madura, R.W. Impey, M.L. Klein, Comparison of simple potential functions for simulating liquid water, *J. Chem. Phys.* 79 (2) (1983) 926–935.
- [33] S. Kanzaki, T. Takahashi, T. Kanno, W. Ariyoshi, K. Shinmyozu, T. Tujisawa, et al., Heparin inhibits BMP-2 osteogenic bioactivity by binding to both BMP-2 and BMP receptor, *J. Cell. Physiol.* 216 (3) (2008) 844–850.
- [34] K.N. Kirschner, A.B. Yongye, S.M. Tschampel, J. González-Outeirino, C.R. Daniels, B.L. Foley, et al., GLYCAM06: a generalizable biomolecular force field. *Carbohydrates, J. Comput. Chem.* 29 (4) (2008) 622–655.
- [35] W.J. Kuo, M.A. Digman, A.D. Lander, Heparan sulfate acts as a bone morphogenetic protein coreceptor by facilitating ligand-induced receptor hetero-oligomerization, *Mol. Biol. Cell* 21 (22) (2010) 4028–4041.
- [36] M.K. Lee, A.D. Lander, Analysis of affinity and structural selectivity in the binding of proteins to glycosaminoglycans: development of a sensitive electrophoretic approach, *Proc. Natl. Acad. Sci. U. S. A.* 88 (7) (1991) 2768–2772.
- [37] J.P. Li, M. Kusche-Gullberg, Heparan sulfate: biosynthesis, structure, and function, *Int. Rev. Cell Mol. Biol.* 325 (2016) 215–273.
- [38] X. Lin, G. Wei, Z. Shi, L. Dryer, J.D. Esko, D.E. Wells, et al., Disruption of gastrulation and heparan sulfate biosynthesis in EXT1-deficient mice, *Dev. Biol.* 224 (2) (2000) 299–311.
- [39] D. Maiolo, S. Federici, L. Ravelli, L.E. Depero, K. Hamad-Schifferli, P. Bergese, Nanomechanics of surface DNA switches probed by captive contact angle, *J. Colloid Interface Sci.* 402 (2013) 334–339.
- [40] L. Mauri, G. Boccardi, G. Torri, M. Karfunkle, E. Macchi, L. Muzi, et al., Qualification of HSQC methods for quantitative composition of heparin and low molecular weight heparins, *J. Pharm. Biomed. Anal.* 136 (2017) 92–105.
- [41] B. Mulloy, M.J. Forster, C. Jones, D.B. Davies, And molecular-modelling studies of the solution conformation of heparin, *Biochem. J.* 293 (Pt.3) (1993) 849.
- [42] B. Ohkawara, Iemura S. Ichiro, P. Ten Dijke, N. Ueno, Action range of BMP is defined by its N-terminal basic amino acid core, *Curr. Biol.* 12 (3) (2002) 205–209.

- [43] R.P. Oomen, N.M. Young, D.R. Bundle, Molecular modeling of antibody–antigen complexes between the brucella abortus o-chain polysaccharide and a specific monoclonal antibody, *Protein Eng. Des. Sel.* 4 (4) (1991) 427–433.
- [44] J.C. Phillips, R. Braun, W. Wang, J. Gumbart, E. Tajkhorshid, E. Villa, et al., Scalable molecular dynamics with NAMD, *J. Comput. Chem.* 26 (16) (2005) 1781–1802.
- [45] M. Poli, D. Girelli, N. Camprostrini, F. Maccarinelli, D. Finazzi, S. Lusciati, et al., Heparin: a potent inhibitor of hepcidin expression in vitro and in vivo, *Blood* 117 (3) (2011) 997–1004.
- [46] M. Poli, M. Asperti, A. Naggi, N. Camprostrini, D. Girelli, M. Corbella, et al., Glycol-split nonanticoagulant heparins are inhibitors of hepcidin expression in vitro and in vivo, *Blood* 123 (10) (2014) 1564–1573.
- [47] M. Poli, M. Asperti, P. Ruzzenenti, L. Mandelli, N. Camprostrini, G. Martini, et al., Oversulfated heparins with low anticoagulant activity are strong and fast inhibitors of hepcidin expression in vitro and in vivo, *Biochem. Pharmacol.* 92 (2014) 467–475.
- [48] M. Poli, M. Asperti, P. Ruzzenenti, A. Naggi, P. Arosio, Non-anticoagulant heparins are hepcidin antagonists for the treatment of anemia, *Molecules* 22 (4) (2017) (pii: E598).
- [49] M. Poli, F. Anower-E-Khuda, M. Asperti, P. Ruzzenenti, M. Gryzik, A. Denardo, et al., Hepatic heparan sulfate is a master regulator of hepcidin expression and iron homeostasis in human hepatocytes and mice, *J. Biol. Chem.* 294 (36) (2019) 13292–13303.
- [50] V.H. Pomin, B. Mulloy, Glycosaminoglycans and proteoglycans, *Pharmaceuticals* 11 (1) (2018) 27.
- [51] C.C. Rider, B. Mulloy, Heparin, heparan sulphate and the TGF- β cytokine superfamily, *Molecules* 22 (5) (2017 Apr 29) 713.
- [52] R. Ruppert, E. Hoffmann, W. Sebald, Human bone morphogenetic protein 2 contains a heparin-binding site which modifies its biological activity, *Eur. J. Biochem.* 237 (1) (1996) 295–302.
- [53] S.A. Samsonov, J.P. Gehrcke, M.T. Pisabarro, Flexibility and explicit solvent in molecular-dynamics-based docking of protein-glycosaminoglycan systems, *J. Chem. Inf. Model.* 54 (2) (2014) 582–592.
- [54] S. Saremba, J. Nickel, A. Seher, A. Kotzsch, W. Sebald, T.D. Mueller, Type I receptor binding of bone morphogenetic protein 6 is dependent on N-glycosylation of the ligand, *FEBS J.* 275 (1) (2008) 172–183.
- [55] S. Von Einem, E. Schwarz, R. Rudolph, A novel TWO-STEP renaturation procedure for efficient production of recombinant BMP-2, *Protein Expr. Purif.* 73 (1) (2010 Sep) 65–69.
- [56] D.O. Wagner, C. Sieber, R. Bhushan, J.H. Börgermann, D. Graf, P. Knaus, BMPs: from bone to body morphogenetic proteins, *Sci. Signal.* 3 (107) (2010) mr1.
- [57] D. Xu, J.D. Esko, Demystifying Heparan sulfate–protein interactions, *Annu. Rev. Biochem.* 83 (2014) 129–157.
- [58] D. Yadin, P. Knaus, T.D. Mueller, Structural insights into BMP receptors: specificity, activation and inhibition, *Cytokine Growth Factor Rev.* 27 (2016) 13–34.